Virtual Inertia Optimization Allocation Based On Grey Wolf Algorithm

Genzhu Wu[1*], Dongliang Nan[1,2], Yu Duan[2], Lu Zhang[2], Ziming Zhu[2], and Xiqiang Chang[1]

[1] School of Electrical Engineering, Xinjiang University, Urumqi 830046, Xinjiang, China
[2] State Grid Xinjiang Electric Power Co., Ltd. Electric Power Science Research Institute, Urumqi 830000, Xinjiang, China
[*] Corresponding author. E-mail: 107552204472@stu.xju.edu.cn

Received: Oct. 17, 2023; Accepted: Jan. 01, 2024

To address the optimal allocation of virtual inertia as a replacement for rotating inertia in power systems, this paper proposes a virtual inertia optimal allocation method. First, the calculation method for determining the minimum inertia requirement of power systems with high penetration of renewable energy is clarified. Next, considering factors like frequency stability and virtual inertia investment costs, a virtual inertia optimization allocation model is constructed with the goals of minimizing the frequency security index and investment costs, subject to constraints such as critical inertia, rate of change of frequency, and maximum frequency deviation. And the grey wolf algorithm is utilized to solve this model. Finally, the modified WSCC 9-bus system and IEEE 39-bus system are simulated to validate the effectiveness and universality of the proposed model in optimally allocating virtual inertia while balancing frequency stability and investment costs.

Keywords: virtual inertia; critical inertia; frequency stability; investment cost; grey wolf algorithm

http://dx.doi.org/10.6180/jase.202411_27(11).0009

1. Introduction

With the vigorous development of new power systems, large-scale wind, photovoltaic and other new energy power generation equipment are gradually replacing traditional synchronous machines in grid connection [1]. However, the random, unstable and weak/no inertia characteristics of wind and photovoltaic power generation pose serious threats to the safety and stability of the operation of new power systems. The power outage incidents in Australia in 2016 and in the United Kingdom in 2019 were both attributed to insufficient system inertia support and frequency regulation capabilities during the occurrence of faults [2].

In recent years, there has been significant development in the field of virtual inertia technology, which utilizes power electronic control to provide new energy sources with inertia support capability [3]. Among these technologies, the most effective in terms of inertia support is the Virtual Synchronous Generator (VSG) [4]. The lacking inertia of new power systems can be compensated by virtual inertia. However, determining the required amount of virtual inertia to be provided by each VSG is a crucial problem that needs to be addressed.

Firstly, we need to determine the total virtual inertia required by the system. Prior to this, we must calculate the critical inertia, which represents the overall inertia demand after the integration of new energy sources. Subsequently, we need to study the allocation of virtual inertia within the grid. The rational allocation of virtual inertia can improve the frequency stability of the power system and also help reduce the investment cost of Virtual Synchronous Generators. Due to the influence of the grid topology and spatial characteristics, different distributions of virtual inertia will have different impacts on the frequency stability of the system [5]. Literature [6] proposed a linear network reduction model of power systems based on the two-norm performance index to consider the inertia location problem, and proposed a solution method through an explicit gradient formula; Literature [7] further considered the robust inertia allocation problem based on this, optimizing according

to the worst-case disturbance location; Literature [8] constructed an objective function based on the two-norm of the Liapunov function and improved the fireworks algorithm to improve the solving performance and accuracy of results; Literature [9] took the maximization of the damping ratio in the maximum oscillation mode as the optimization objective, and took the related parameters in the control method of virtual inertia as optimization variables, and constructed the optimal distribution model of virtual inertia under the constraints of frequency security and stability, and adopted the Newton method as the solving method; Literature [10] established a second-order mathematical model of power systems for small disturbance analysis, considering the related parameters of virtual inertia, taking the two-norm Liapunov function as the objective function to seek the influence of inertia configuration on the frequency stability of the system, and proposed the centroid interpolation optimization algorithm of Voronoi diagram; Literature [11] numerically solved the problem of virtual inertia and damping allocation between inverters in power grids, using semidefinite programming relaxation to solve non-convex problems, and proposed an embedded feasibility distributed method within the alternating direction multiplier framework.

In summary, the mechanism of how the distribution of virtual inertia in the system affects frequency is quite complex, and existing literature has not fully studied it. Moreover, most literature does not consider the cost issue of virtual inertia provided by distributed energy resources. Therefore, this paper proposes an optimization allocation method of virtual inertia that considers investment cost issues. First, the critical inertia of the power system is calculated by swing equations. Then considering grid frequency indicators and cost factors, an optimization allocation model of virtual inertia is constructed, and the gray wolf algorithm is used to solve the optimal solution of this model. Finally, simulations are carried out on the modified WSCC 9-bus model and IEEE39-bus model for verification.

2. Critical inertia

2.1. Inertia and Power System Frequency Safety

The inertial response of a power system is to resist frequency changes caused by external disturbances. It can slow down the speed of system frequency changes and is an important factor in ensuring frequency stability of the system. The inertia constant H is generally used to characterize the size of the generator's inertia, which represents the ratio of the generator's kinetic energy E_K at rated speed to its rated power S_b [12]:

$$H = \frac{E_{\mathrm{K}}}{S_{\mathrm{b}}} \tag{1}$$

When a power system is subjected to a disturbance, inertial response is the system's first reaction. According to the swing equation, during this process, the kinetic energy stored in the synchronous machine is converted into inertial support power, which is always equal to the deviation between mechanical power and electromagnetic power [13]:

$$2H\frac{df}{dt} = P_{\mathrm{m}} - P_{\mathrm{e}} - D\Delta f \tag{2}$$

where H is the generator's inertial time constant; f is the generator frequency; P_{m} is the generator mechanical power; P_{e} is the generator electromagnetic power; D is the generator damping coefficient; Δf is the deviation between the generator frequency and rated frequency.

Therefore, inertia plays an important role in maintaining the safe and stable operation of the system. It can provide frequency support when faults occur in the power system, slow down the rate of change of system frequency, and buy time for primary frequency control, which is an indispensable link in maintaining the frequency stability of the power system.

2.2. Method for Calculating Critical Inertia of Power Systems

For a synchronous machine, according to the swing equation, the mathematical model of its frequency change during the inertial support period can be obtained. The frequency response of a power system after a contingency can be divided into three time scales: inertial response, primary frequency control (PFC), and secondary frequency control (SFC). During the inertial response, frequency control is not actively involved, and the damping effect is relatively small compared to the inertia effect. The frequency characteristics of the power network are primarily influenced by the system's inertia. Thus, when calculating the inertial time constant, damping can be disregarded. And Eq. (2) can be transformed into Eq. (3).

$$\frac{df}{dt} = \frac{P_{\mathrm{m}} - P_{\mathrm{e}}}{2H} \tag{3}$$

Integrating both sides of the equation with respect to time gives:

$$f = \int \frac{P_{\mathrm{m}} - P_{\mathrm{e}}}{2H} dt + C = \frac{1}{2H}\int \Delta P dt + C \tag{4}$$

where ΔP is the imbalance power at the generator node after disturbance; C is the constant term after integration.

Then considering the mathematical model of the overall frequency change of the power grid, assume there are p synchronous generators and q virtual synchronous machines in the entire power grid. Since virtual synchronous machines also use the swing equation to provide inertial support to the system, their frequency change during the inertial support stage can also be represented by Eq. (4). Therefore, when considering the entire power system, Eq. (4) can be expanded to:

$$f_{\text{coi}} = \frac{1}{2H_{\text{sys}}} \sum_{i=1}^{p+q} \int \Delta P_i dt + C \tag{5}$$

where f_{coi} is the frequency at the center of inertia in the power grid; $H_{\text{sys}}$is the system inertia constant; ΔP_i is the imbalance power at each generator node.

When measuring frequency stability during a disturbance, RoCoF and frequency extremes are key metrics [14]. China's power system generally uses the maximum frequency deviation after a fault disturbance as a constraint condition. Therefore, this section focuses on studying the impact of frequency extremes on critical inertia after a disturbance. The calculation method for frequency deviation is shown as follows:

$$\Delta f = f_{\text{coi}} - f_o \tag{6}$$

where f_o is the Rated frequency.

And Eq. (5) can be transform to Eq. (7):

$$H_{\text{sys}} = \frac{\sum_{i=1}^{p+q} \int \Delta P_i dt}{2f_{\text{coi}} - C} \tag{7}$$

Combining Eqs. (6) and (7), the mathematical model of the equivalent inertia constant at this stage can be obtained as:

$$H_{\text{sys}} = \frac{\sum_{i=1}^{p+q} \int \Delta P_i dt}{2\left(\Delta f + f_0 - C\right)} \tag{8}$$

where Δf_{coi} is the maximum frequency deviation at the inertia center, f_0 is the rated frequency of the power system.

By the above equation, when the maximum frequency deviation Δf_{coi} is known, the minimum required rotational inertia of the power system, referred to as the critical inertia , $H_{\text{sys,min}}$ can be obtained:

$$H_{sys,\text{min}} = \frac{\sum_{i=1}^{m+n} \int \Delta P_i dt}{2\left(\Delta f_{\text{max}} + f_0 - C\right)} \tag{9}$$

3. Model for optimizing allocation of virtual inertia

When the inertia provided by synchronous generators in the power system cannot meet the system's requirements, virtual inertia support needs to be provided by new energy sources to maintain the safe and stable operation of the power system. The inertia at different nodes of the power grid is different and has different influence on the frequency recovery ability of the system after failure. This paper establishes an optimization allocation model for virtual inertia to reasonably allocate virtual inertia and enhance the system's disturbance resistance capability. This section will introduce the virtual inertia optimization allocation model from three aspects: the objective function, constraints, and optimization algorithm.

3.1. Objective function

The primary objective of optimally allocating virtual inertia in this paper is to enhance the system's disturbance resistance capability and improve system stability. Literature [15] proposed the Frequency Security Index (FSI) to quantitatively evaluate the frequency security (including transient and steady-state) of a power system under specific operating conditions, with quantitative definitions of unsafe, safe and absolutely safe boundaries as shown in Table 1. This paper only considers the impact of inertia on system frequency characteristics and focuses on frequency metrics during transient processes, i.e. rate of change of frequency and maximum frequency deviation.

Table 1. Frequency index.

Indicators	Absolute safety	Safety	Unsafe
Δf	$\alpha_{\text{min}} \cdot \Delta f_{\text{max}}$	$\alpha \cdot \Delta f_{\text{max}}$	Δf_{max}
$\lvert\text{RoCoF}\rvert$	$\beta_{\text{min}} \cdot \text{RoCoF}_{\text{max}}$	$\beta \cdot \text{RoCoF}_{\text{max}}$	$\text{RoCoF}_{\text{max}}$

China has detailed provisions for the maximum frequency deviation during frequency dynamic processes based on the three-level verification standards for frequency stability in engineering simulations [16]. However, China does not have corresponding provisions for RoCoF during frequency dynamic processes. Therefore, this paper refers to the provisions in literature [17] to set the unsafe, safe and absolutely safe boundaries for RoCoF. The final FSI boundary parameters are shown in Table 2.

Table 2. FSI parameter.

Parameters	Numerical	Parameters	Numerical
$\Delta f_{\text{max}}(\text{Hz})$	0.6	α_{min}	0.2
$\text{RoCoF}_{\text{max}}(\text{Hz/s})$	1.0	β_{max}	0.9
α_{max}	0.9	β_{min}	0.2

The overall calculation process of FSI is shown in Fig. 1, which clearly shows the inputs, calculation process and outputs of FSI.

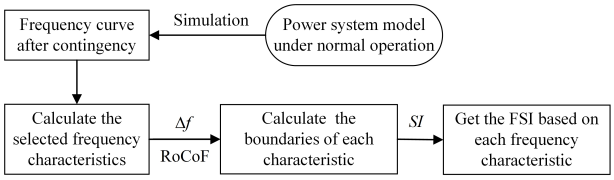

Fig. 1. FSI calculation process.

In addition, considering the economic factors of virtual inertia optimal allocation, the energy sources and methods for distributed energy resources to provide virtual inertia have some differences, and the costs will accordingly have some differences. Therefore, considering the investment cost of equipment, simplifying the cost of different types of distributed energy into different cost coefficients. The investment cost function is shown below:

$$C_{\mathrm{H}} = C_1 \sum H_n + C_2 \sum H_m + C_3 \sum H_l \tag{10}$$

where C_{H} is the total investment cost required for providing the total virtual inertia.; $\sum H_n$ and C_1 are the total virtual inertia provided by n storage power stations and its corresponding cost coefficient; $\sum H_m$ and C_2 are the total virtual inertia provided by m photovoltaic power stations and its corresponding cost coefficient; $\sum H_l$ and C_3 are the total virtual inertia provided by l wind farms and its corresponding cost coefficient.

In summary, the objective function of the virtual inertia optimization allocation model constructed in this paper consists of two parts: the FSI of the wind farm system and the investment cost function. In order to carry out unified optimization processing, both are normalized to obtain the following objective function:

$$\min F = a\left(\frac{\Delta f}{\Delta f_{\max}} + \frac{f_{\mathrm{RoCoF}}}{RoCoF_{\max}}\right) + b\frac{C_{\mathrm{H}}}{\sum H_m + \sum H_n + \sum H_l} \tag{11}$$

where a represents the weight of FSI in the objective function; b represents the weight of investment cost in the objective function; $\Delta f_{\max}$ is the critical value of the maximum frequency deviation unsafe in Table 1; $\mathrm{RoCoF}_{\max}$ is the critical value of the rate of change of frequency unsafe in Table 1.

3.2. Constraint conditions

Combining the critical inertia in Chapter 1 and the objective function constructed in the previous section, constraints will be imposed on the total virtual inertia, maximum frequency deviation, and RoCoF, so that the solution of the objective function can better conform to the actual situation.

3.2.1. *Virtual inertia constraint*

According to reference [18], the total inertia of the new power system can be calculated by the following formula, assuming there are i synchronous machines and j virtual synchronous machines:

$$H_{\mathrm{sys}} = \frac{\sum H_i S_i + \sum H_j^{\mathrm{vl}} S_j}{\sum S_i + \sum S_j} \tag{12}$$

where H_i represents the inertia constant of synchronous machine i; S_i represents the capacity of synchronous machine; H_j^{vl} represents the inertia constant of virtual synchronous machine; S_j represents the capacity of virtual synchronous machine.

To ensure safe and stable operation of system frequency, the total system inertia should be greater than the critical inertia. The total system inertia consists of the inertia of traditional synchronous machines and the virtual inertia provided by virtual synchronous machines. The inertia of traditional synchronous machines is fixed, while the virtual inertia is generated by simulating the swing equation of synchronous machines through controlling power electronic devices, and its size can be adjusted. Therefore, when the rotational inertia of synchronous machines is insufficient to meet the system requirements, the virtual inertia can be adjusted to satisfy the inertia needs of the system. Combining Eq. (7) and Eq. (10), the total virtual inertia should satisfy the following condition:

$$\sum H_j^{\mathrm{vl}} S_j = H_{\mathrm{sys}}\left(\sum S_i + \sum S_j\right) - \sum H_i S_i \geq H_{\mathrm{sys,min}} \sum S_j \tag{13}$$

3.2.2. *Maximum frequency deviation constraint*

After the system is disturbed by faults, the maximum frequency deviation and RoCoF of grid inertia are generally used as parameters to judge whether the system frequency is stable. Whether the third line of defense high-frequency tripping device is activated depends on the maximum frequency deviation value. To avoid triggering the high-frequency tripping device, and considering China's regulations on the maximum system frequency deviation, the maximum frequency deviation of the system needs to satisfy the following constraint condition:

$$|\Delta f| \leq \Delta f_{\max} \tag{14}$$

3.2.3. *RoCoF constraint*

The RoCoF is related to the scale of the fault disturbance and the size of the system inertia. Whether the RoCoF relay protection device operates also depends on the magnitude of the RoCoF. Therefore, in order to avoid triggering the RoCoF relay protection device, the RoCoF should be less than the maximum value specified by the system, that is:

$$\mathrm{RoCoF} = \frac{\Delta P f_0}{2H_{\mathrm{sys}}} \leq \mathrm{RoCoF}_{\max} \tag{15}$$

Finally, the Optimization model is shown in Eq. (16).

$$\begin{aligned} \text{Minimize} \quad & F = a\left(\frac{\Delta f}{\Delta f_{\max}} + \frac{f_{\mathrm{RoCoF}}}{\mathrm{RoCoF}_{\max}}\right) + b\frac{C_{\mathrm{H}}}{\sum H_m + \sum H_n + \sum H_l} n \\ \text{subject to:} \quad & \sum H_j^{\mathrm{vl}} S_j \geq H_{\mathrm{sys\ min}} \sum S_j \\ & |\Delta f| \leq \Delta f_{\max} n \\ & \mathrm{RoCoF} \leq \mathrm{RoCoF}_{\max}\, n \end{aligned} \tag{16}$$

3.3. Grey wolf algorithm

The objective function of the virtual inertia optimization allocation model is highly non-convex, and traditional convex optimization algorithms can hardly effectively solve this problem. However, in recent years, swarm intelligence algorithms have been widely recognized as an effective method to solve non-convex optimization problems. Among them, the GWO algorithm solves optimization problems by simulating the social behaviors, collaborative cooperation and search strategies among grey wolf individuals [19]. Compared with other optimization algorithms, the grey wolf algorithm has stronger search ability and faster convergence speed, and is easy to implement. Therefore, it has strong practical value and application prospects in the optimization of practical problems [20].

The flowchart of using the grey wolf optimization algorithm to solve the virtual inertia optimization allocation model is shown in Fig. 2.

Where the target position of the wolf pack and the position calculation formula of the search population are shown below [19]:

$$\boldsymbol{D} = \left|\boldsymbol{C} \cdot \boldsymbol{X}_p(t) - \boldsymbol{X}(t)\right| \tag{17}$$

$$\boldsymbol{X}(t+1) = \boldsymbol{X}_p(t) - \boldsymbol{A} \cdot \boldsymbol{D} \tag{18}$$

where t represents the current iteration; $\boldsymbol{A}$ and $\boldsymbol{C}$are coefficients to be calculated [20]; $\boldsymbol{X}_p$ is the position vector of the prey; $\boldsymbol{X}(t)$ is the current position vector of the wolf pack; $\boldsymbol{X}(t+1)$ represents the next position vector of the grey wolf.

The coefficient vectors $\boldsymbol{a}$, $\boldsymbol{A}$ and $\boldsymbol{C}$ can be determined by the following formulas [20]:

$$\boldsymbol{a}(t) = 2(1 - t/M) \tag{19}$$

$$\boldsymbol{A} = 2\boldsymbol{a} \cdot \boldsymbol{r}_1 - \boldsymbol{a} \tag{20}$$

$$\boldsymbol{C} = 2 \cdot \boldsymbol{r}_2 \tag{21}$$

where $\boldsymbol{a}$ will decrease linearly from 2 to 0 during cyclic iterations; $\boldsymbol{r}_1$ and $\boldsymbol{r}_2$ are randomly generated vectors from [0,1]; M is the final number of iterations set.

4. Simulation experiment and analysis

In order to verify the effectiveness of the virtual inertia optimization allocation model constructed in this paper, the model code was written in python, and experiments were conducted on the modified WSCC 9-bus system and IEEE 39 bus system. All simulation models and results were obtained using the power system analysis software tool Dome [21].

4.1. WSCC 9-bus system

The single-line diagram of the modified WSCC 9-bus system is shown in Fig. 3. In this paper, the original synchronous machines G2 and G3 in the WSCC 9-bus system are replaced with two virtual synchronous machines VSG1 and VSG2.

The synchronous machine models in the system are fourth order two axis models, equipped with Turbine Governors (TG) and Automatic Voltage Regulators (AVR). Both VSG use nonlinear state space models. In addition, a static VAR compensator is installed on system bus 8.

The data of the 3 generators in the simulation model are shown in Table 3. The data of WSCC 9-Bus System can be found in reference [22]. The active power output of each device is represented by per unit(pu), with a base value of 100MW. Except for buses 1, 2, and 3, the bus voltages of the remaining buses are 230kV. The inertia constant H of synchronous machine G1 is set to 23.64 MWs/MVA, and the initial inertia constants of the two VSG are set to 0.1. More detailed parameters of the simulation model can also be found in reference [22]. In addition, it is assumed that VSG1 and VSG2 represent energy storage stations and photovoltaic power stations respectively, and the investment cost coefficients of virtual inertia C1:C2 = 1:1.1.

In the experiment, considering the balance between solving speed and result accuracy, after multiple simulation experiments and calculations, when the population size of the grey wolf algorithm is set to 20 and the maximum number of iterations is set to 50, a satisfactory optimal solution can be obtained. In this experiment, according to the

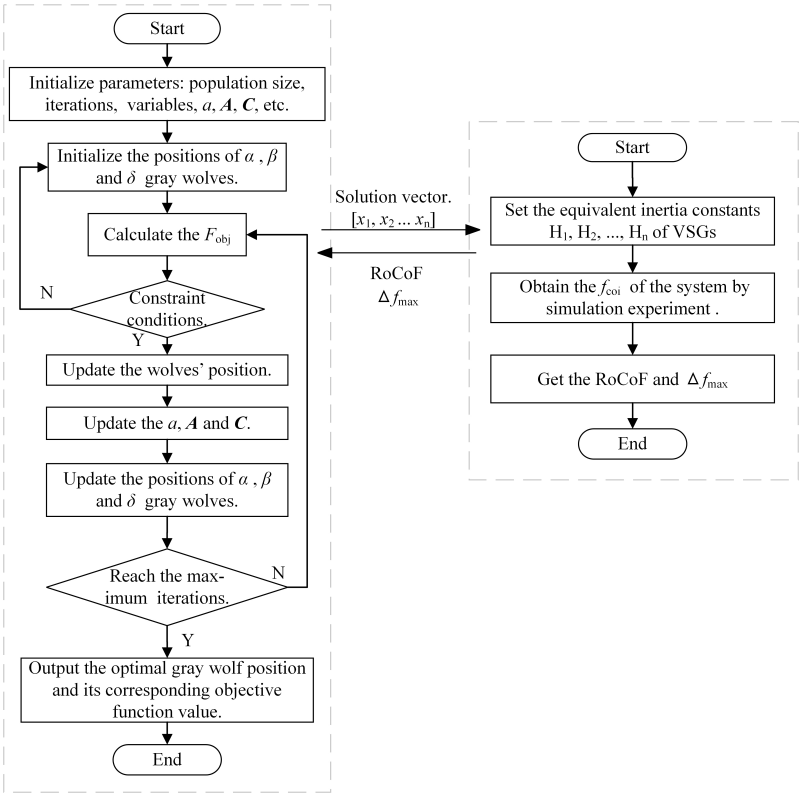

Fig. 2. GWO calculation process.

Table 3. FSI parameter.

Equipment	Rated voltage/kV	Parameters/pu	Numerical/MW
G1	16.5	0.8	247.5
VSG1	18.0	1.63	192
VSG2	13.8	0.85	128

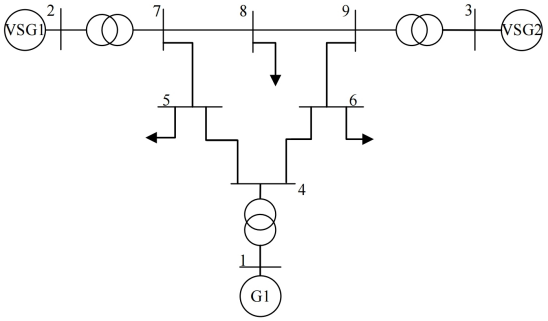

Fig. 3. Modified WSCC 9-Bus System.

limitations of the rate of change of frequency and the maximum frequency deviation, considering that the system has a power shortage of 45MW due to sudden load increase, the convergence curve of the objective function F of the virtual inertia optimization allocation model obtained experimentally is shown in Fig. 4. Table 4 shows some data of the optimal inertia constant values, RoCoF and maximum frequency deviation of VSG1 and VSG2 at each iteration during the experiment.

We chose ten different optimization algorithms to solve the model constructed in this paper. The 10 algorithms are ABO(Artificial Bee Colony Optimizer), AFS(Artificial Fish Swarm Algorithm), DE(Differential Evolution), FA (Fireworks algorithm), GA (Genetic Algorithm), GWO (Grey Wolf Optimizer), GSA (Gravitational Search Algorithm), HS (Harmony Search), PSO (Particle Swarm Optimization), SA (Simulated Annealing). The experimental results are displayed in Fig. 4 and Fig. 5. Fig. 4 shows the iterative process of these 10 algorithms and Fig. 5 shows the solution time of these 10 algorithms. Thus, considering the solving speed and solving accuracy, we have chosen the gray wolf algorithm.

It can be seen from Table 4 that the model has the opti-

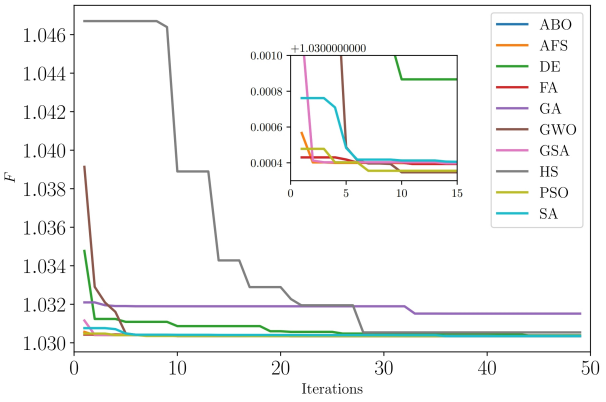

Fig. 4. The iterative process for each algorithm.

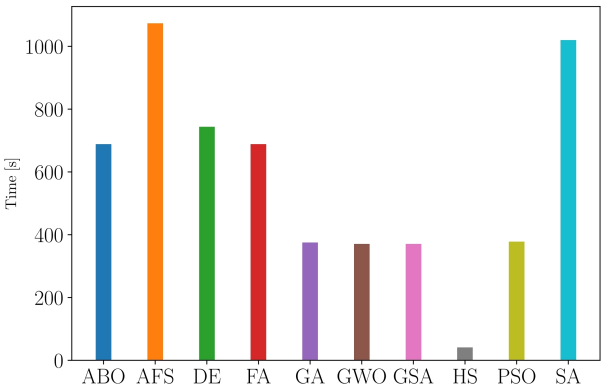

Fig. 5. The Solution time for each algorithm.

mal solution when the equivalent inertia constants of VSG1 and VSG2 are 80s and 24.4s. And the virtual inertia optimization allocation model constructed in this paper fully considers the investment cost of virtual inertia, and the RoCoF is within the absolutely safe range and the maximum frequency deviation is within the safe range when the optimal solution is obtained.

Table 5 compares the optimisation model proposed in this paper with existing optimisation models. The objective function of the optimization model of the existing research only focuses on the aspect of system frequency stability, without considering the economic factor of virtual inertia. And the grid model used in the simulation is relatively simple. The optimization model in this paper not only ensures the safety and stability of the system frequency through two specific indexes, namely, RoCoF and frequency deviation, but also makes a preliminary exploration of the cost factor of virtual inertia. And the grey wolf algorithm can be guaranteed in solving speed and accuracy compared to other algorithms. The model has ultimately verified by the WSCC 9 and IEEE 39 systems, and the simulation results show that show that the model has excellent general applicability.

4.2. IEEE39 bus system

This section verifies the versatility of the virtual inertia optimization model proposed in this paper through simulation experiments on the modified IEEE 39-bus system. The system single-line diagram is shown in Fig. 6.

In this paper, the 5 traditional synchronous machines on buses 5, 6, 7, 8, and 10 are replaced with 5 virtual synchronous machines. The data of the 10 generators in the simulation model are shown in Table 5. The data of IEEE39-bus system can be found in reference [22]. The voltage amplitude and active power output of each generator are represented by per unit (pu), with the rated voltage base value specified as 345kV and the active power base value as 100MW. Except for the generator buses, the rated voltage of other buses is 345kV.

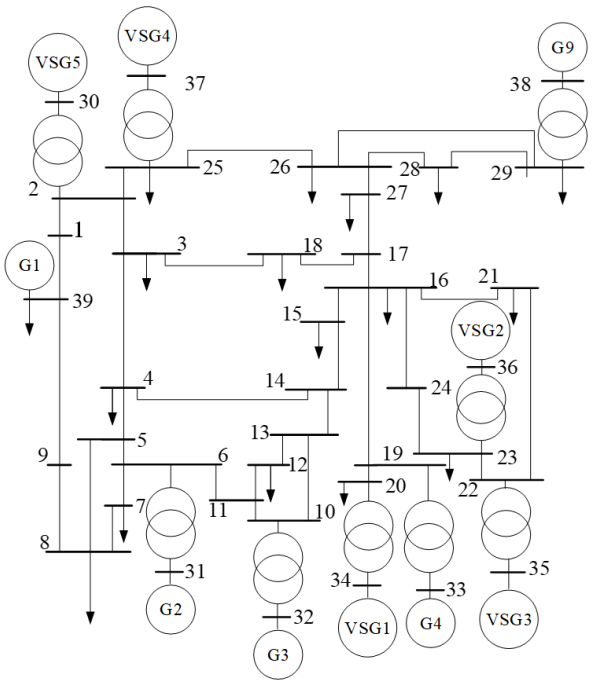

Fig. 6. Modified IEEE39 Bus System.

The inertia constants H of synchronous machines G1, G2, G3, G4 and G9 are set to 500, 30.3, 35.8, 28.6 and 34.5 MWs/MVA respectively, and the initial inertia constants of the 5 VSG are set to 1. More detailed parameters of the simulation model can be found in reference [22]. In addition, it is assumed that among the 5 VSG, VSG1 is an energy storage power station, VSG2 and VSG3 are photovoltaic power stations, and VSG4 and VSG5 are wind farms, with the virtual inertia investment cost coefficient

Table 4. Process of optimal solution change.

Iterative times	Optimal solution	RoCoF(Hz/s)	Maximum frequency deviation(Hz)
1	[77.4, 3.9]	0.092	0.442
5	[80, 27.3]	0.082	0.421
10	[80, 24.4]	0.086	0.432
15	[80, 24.4]	0.088	0.432
20	[80, 24.4]	0.088	0.432
25	[80, 24.4]	0.086	0.432
30	[80, 24.4]	0.086	0.432

Table 5. Comparison of various virtual inertia allocation methods.

Methods	Objective function	Solution method
Literature [6][7]	The 2-norm of Lyapunov function	Explicit gradient equation
Literature [8]	The 2-norm of Lyapunov function	Fireworks algorithm
Literature [9]	Damping ratio	The Newtonian method
Literature [10]	The 2-norm of Lyapunov function	Voronoi diagram Algorithm
Model of this paper	Frequency deviation + RoCoF+ Cost	Grey Wolf Optimizer

Table 6. Parameters of Equipments.

Equipment	Voltage amplitude/pu	Parameters/pu	Capacity/pu
G1	1.03	10.0	1.0
G2	0.982	5.1	1.0
G3	0.983	6.5	1.0
G4	0.997	6.32	1.0
VSG5	1.012	5.1	1.0
VSG6	1.049	6.5	1.0
VSG7	1.064	5.6	1.0
VSG8	1.028	5.4	1.0
G9	1.027	8.3	1.0
VSG10	1.048	2.5	1.0

ratio C1:C2:C3=1:1.1:1.2.

In this simulation experiment, the population size of the grey wolf algorithm was 20, and the maximum number of iterations was 50. The convergence curve of the objective function F of the obtained virtual inertia optimization allocation model is shown in Fig. 7. Table 7 shows partial data of the optimal inertia constant values, RoCoF and maximum frequency deviation of the 5 VSG after each iteration.

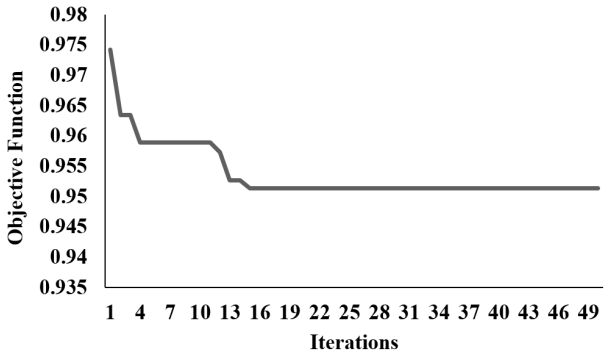

Fig. 7. IEEE39 bus system objective function.

According to Fig. 7, the virtual inertia optimization allocation model established in this paper also performs well when facing a complex system. According to Table 7, when the equivalent inertia constants of VSG1, VSG2, VSG3, VSG4 and VSG5 are 90.5s, 38.6s, 17.2s, 1.2s and 4.9s, the model has the optimal solution. It has achieved a relatively optimal result after 25 iterations, and the convergence speed and computational accuracy are both good.

As can be seen from Table 7, the virtual inertia optimization allocation model established in this paper fully considers the investment cost problem of virtual inertia provided by different types of distributed energy resources when facing complex power systems such as IEEE39. The maximum frequency deviation is within the safe range, RoCoF is in the absolutely safe range, enhancing the system's ability to resist interference and leaving more room for adjustment when the system is disturbed.

5. Conclusion

To solve the problem of virtual inertia allocation of new energy, this paper establishes a virtual inertia optimization

Table 7. Process of optimal solution change.

Iterative times	Optimal solution	RoCoF(Hz/s)	$\Delta f_{max}(Hz)$	F_{obj}
1	[77.7, 98.6, 28.9, 8.6, 84.9]	0.047	0.478	0.9742
5	[89.9, 49.1, 79.1, 11.4, 3.1]	0.050	0.480	0.9589
10	[89.9, 49.1, 79.1, 11.4, 3.1]	0.050	0.480	0.9589
15	[94.9, 10.9, 46.3, 8.9, 2.5]	0.051	0.482	0.9526
20	[90.5, 38.6, 17.2, 1.2 4.9]	0.052	0.483	0.9513
25	[90.5, 38.6, 17.2, 1.2 4.9]	0.052	0.483	0.9513
30	[90.5, 38.6, 17.2, 1.2 4.9]	0.052	0.483	0.9513

allocation model. This model fully considers economic factors and frequency stability, with the objectives of minimizing frequency security index and cost, and system critical inertia, RoCoF and maximum frequency deviation as constraints. To solve this model, the grey wolf algorithm is used as the solution algorithm, which has advantages such as easy implementation, fast solution and high solution accuracy.

In summary, the experimental results finally show that the virtual inertia optimization allocation model established in this paper can effectively allocate virtual inertia while considering investment costs, thus improving the frequency stability of the system. The model also performs well on complex power systems, demonstrating strong generalizability. Future research can further take into account the spatiotemporal characteristics of the power grid and more accurately estimate the investment costs of virtual inertia to establish an even more precise model. In our future research, we will delve deeper into the temporal and spatial characteristics of the grid. We aim to accurately estimate the investment cost associated with virtual inertia and develop a systematic approach to calculate the investment cost coefficient of virtual inertia. By doing so, we will construct an enhanced optimization model for the allocation of virtual inertia, resulting in more precise and effective outcomes.

Acknowledgments

This paper is funded by the Science and Technology Project of State Grid Xinjiang Electric Power Co., Ltd. Electric Power Science Research Institute (No. 5230DK230001).

References

[1] K. B. Kiran, M. Indira, R. Nagaraja, et al., (2021) *"Mathematical modeling and evaluation of performance characteristics of a hybrid solar PV and wind energy system"* **Journal of Applied Science and Engineering *25***(4): 785–797. DOI: 10.6180/jase.202208_25(4).0014.

[2] K. Prabhakar, S. K. Jain, and P. K. Padhy, (2022) *"Inertia estimation in modern power system: A comprehensive review"* **Electric Power Systems Research *211***: 108222. DOI: 10.1016/j.epsr.2022.108222.

[3] D. Sun, H. Liu, S. Gao, L. Wu, P. Song, and X. Wang, (2020) *"Comparison of Different Virtual Inertia Control Methods for Inverter-based Generators"* **Journal of Modern Power Systems and Clean Energy** *8*(4): 768–777. DOI: 10.35833/MPCE.2019.000330.

[4] M. Chen, D. Zhou, and F. Blaabjerg, (2020) *"Modelling, Implementation, and Assessment of Virtual Synchronous Generator in Power Systems"* **Journal of Modern Power Systems and Clean Energy** *8*(3): 399–411. DOI: 10.35833/MPCE.2019.000592.

[5] D. Li, Q. Wang, X. Zhang, T. Wang, and W. Hou, (2023) *"Inertia Configuration Method to Enhance Frequency Stability of Power Grids Considering the Spatial Distribution Characteristics"* **IET Conference Proceedings *2023***(15): 1270–1275. DOI: 10.1049/icp.2023.2485.

[6] B. K. Poolla, S. Bolognani, and F. Dörfler. "Placing Rotational Inertia in Power Grids". In: *2016 American Control Conference (ACC)*. 2016, 2314–2320. DOI: 10.1109/ACC.2016.7525263.

[7] B. K. Poolla, S. Bolognani, and F. Dörfler, (2017) *"Optimal Placement of Virtual Inertia in Power Grids"* **IEEE Transactions on Automatic Control *62***(12): 6209–6220. DOI: 10.1109/TAC.2017.2703302.

[8] H. B. Liu, H. Ma, Z. Z. Xiong, and X. X. Tian, (2019) *"Virtual Inertia Configuration Strategy Based on Improved Fireworks Algorithm"* **Science Technology and Engineering *19***(154-158):

[9] J. K. Huang, Z. F. Yang, J. L. Liu, J. Yu, and J. Ren, (2020) *"Optimal Allocation of Virtual Inertia for Improving Small-signal Stability"* **Proceedings of the CSEE *40***(713-723): DOI: 10.13334/j.0258-8013.pcsee.190887.

[10] H. B. Liu. *"Virtual inertia configuration based on multi-objective optimization"*. (mathesis). China Three Gorges University, 2021.

[11] T. Han and D. J. Hill, (2021) *"Dispatch of virtual inertia and damping: Numerical method with SDP and ADMM"* **International Journal of Electrical Power & Energy Systems *133***: 107259.

[12] F. Zeng, J. Zhang, G. Chen, Z. Wu, S. Huang, and Y. Liang, (2020) *"Online Estimation of Power System Inertia Constant Under Normal Operating Conditions"* **IEEE Access *8***: 101426–101436. DOI: 10.1109/ACCESS.2020.2997728.

[13] M. Liu, J. Chen, and F. Milano, (2021) *"On-Line Inertia Estimation for Synchronous and Non-Synchronous Devices"* **IEEE Transactions on Power Systems *36***(3): 2693–2701. DOI: 10.1109/TPWRS.2020.3037265.

[14] X. Deng, R. Mo, P. Wang, J. Chen, D. Nan, and M. Liu, (2023) *"Review of RoCoF Estimation Techniques for Low-Inertia Power Systems"* **Energies *16***(9): DOI: 10.3390/en16093708.

[15] H. Delkhosh and H. Seifi, (2021) *"Power System Frequency Security Index Considering All Aspects of Frequency Profile"* **IEEE Transactions on Power Systems *36***(2): 1656–1659. DOI: 10.1109/TPWRS.2020.3047510.

[16] Y. Z. Xie. *"Power system frequency stability mechanism and coordination control with large frequency deviation scenario"*. (phdthesis). Shandong University, 2021.

[17] A. Pepiciello and A. Vaccaro. "An Optimization-based Method for Estimating Critical Inertia in Smart Grids". In: *2019 IEEE International Conference on Systems, Man and Cybernetics (SMC)*. 2019, 2237–2241. DOI: 10.1109/SMC.2019.8914156.

[18] Y. Liu, Q. Zhao, and D. Liang. "Inertia Characteristic Analysis and Inertia Estimation of New Energy Power System". In: *2022 IEEE/IAS Industrial and Commercial Power System Asia (I&CPS Asia)*. 2022, 1350–1355. DOI: 10.1109/ICPSAsia55496.2022.9949746.

[19] S. Mirjalili, S. Saremi, S. M. Mirjalili, and L. dos S. Coelho, (2016) *"Multi-objective grey wolf optimizer: A novel algorithm for multi-criterion optimization"* **Expert Systems with Applications *47***: 106–119. DOI: 10.1016/j.eswa.2015.10.039.

[20] F. Wang, C. Chen, H. Zhang, Y. Ma, et al., (2022) *"Short-term Load Forecasting Based On Variational Mode Decomposition And Chaotic Grey Wolf Optimization Improved Random Forest Algorithm"* **Journal of Applied Science and Engineering *26***(1): 69–78.

[21] F. Milano. "A python-based software tool for power system analysis". In: *2013 IEEE Power and Energy Society General Meeting*. 2013, 1–5. DOI: 10.1109/PESMG.2013.6672387.

[22] F. Milano. *Power system modelling and scripting*. Springer Science & Business Media, 2010.